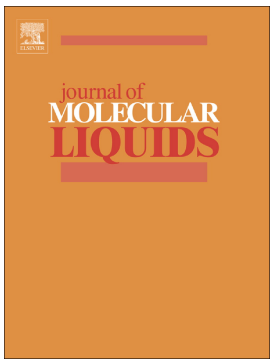


# Three in one: Mesogenic aromatic acid as a liquid crystal matrix, a chiral dopant in liquid crystals and a stabilizer for nanoparticles

A.S. Merekalov, G.A. Shandryuk, V.S. Bezborodov, O.A. Otmakhova, S.G. Mikhalyonok, N.M. Kuz'menok, A.S. Arol, M.A. Osipov, R.V. Talroze

PII: S0167-7322(18)35122-5
DOI: https://doi.org/10.1016/j.molliq.2018.12.036
Reference: MOLLIQ 10112

To appear in: *Journal of Molecular Liquids*

Received date: 15 October 2018
Revised date: 30 November 2018
Accepted date: 5 December 2018

Please cite this article as: A.S. Merekalov, G.A. Shandryuk, V.S. Bezborodov, O.A. Otmakhova, S.G. Mikhalyonok, N.M. Kuz'menok, A.S. Arol, M.A. Osipov, R.V. Talroze , Three in one: Mesogenic aromatic acid as a liquid crystal matrix, a chiral dopant in liquid crystals and a stabilizer for nanoparticles. Molliq (2018), https://doi.org/10.1016/j.molliq.2018.12.036

# Three in one: mesogenic aromatic acid as a liquid crystal matrix, a chiral dopant in liquid crystals and a stabilizer for nanoparticles.

A.S. Merekalov[a], G.A. Shandryuk[a], V.S. Bezborodov[b], O.A. Otmakhova[a] , S.G. Mikhalyonok[b], N.M. Kuz'menok[b], A.S. Arol[b], M.A. Osipov[c, a], R.V. Talroze[a]

[a]*A.V.Topchiev Institute of Petrochemical Synthesis, RAS, 119991, Moscow, Leninsky prospect 29, Russia*

[b] *Department of Organic Chemistry, Belarusian State Technological University, 220006, Minsk, Belarus;*

[c]*Department of Mathematics, University of Strathclyde, Glasgow G1 1XH, UK*

Correspondence details: Institute of Petrochemical Synthesis, Russian Academy of Sciences, 29 Leninsky prospect, 119991 Moscow Russia

e-mail: rtalroze@ips.ac.ru



## Abstract

Studies of thermodynamics of the N*-I phase transitions and optical properties of the new liquid crystal - (*R*)-2-[4"-(*trans*-4-butylcyclohexyl)-2'-chloro-*p*-terphenyl-4-oxy) propanoic acid are carried out. The aim of these studies is to analyse the capabilities of that liquid crystal to simultaneously serve as a matrix for inorganic semiconductor nanoparticles (NP) as well as a chiral dopant for liquid crystals and a chiral ligand

stabilizing the surface of CdSe NPs. The chiral doping of a nematic liquid crystal was proven by the measurements of selective transmittance of the visible light. The embedding of NPs in a nematic liquid crystal leads to the increase in $T_{N^*I,}$ which is explained by the shape anisotropy of the NPs. The anisotropy of the ligand shell may result from the interaction between the ligand and LC matrix inducing the change of the spherical shape of the shell toward the ellipsoidal one. $T_{N^*I}$ of the liquid crystal matrix of (*R*)-2-[4”-(*trans*-4-butylcyclohexyl)-2’-chloro-*p*-terphenyl-4-oxy) propanoic acid (R-MPA) decreases with the embedding of NPs stabilized by the same ligands, which is in a good agreement with prior experimental results and theory, but there exists a considerable quantitative difference.

**Introduction**

The development of new materials allows for creating composites that combine properties of liquid crystals (LCs) and inorganic nanoparticles (NPs). An application of NPs as dopants for modulating LC properties is one of the major trends of the modern science related to liquid crystals. In addition to some quantitative characteristics of LCs such as threshold voltage, elastic constants and switching times of electro-optical effects known in liquid crystals [1-6], NPs may also affect nematic-to-isotropic phase transitions. The decrease in the $T_{NI}$ transition temperature is observed in nematics doped with NPs of silver [7- 10], gold [11] and $SiO_2$ [12, 13]. That effect is explained by Gorkunov and Osipov [14] as the dilution one. The above mentioned decrease in $T_{NI}$ transition temperature is characteristic for NPs having isotropic shape whereas the

increase in the temperature is observed when strongly anisotropic NPs are embedded in liquid crystals [12, 13]. Many of those effects are interpreted by a molecular theory which is presented in [11, 14].

It is necessary to note that the majority of known examples of NPs dispersions in liquid crystals do not show sufficient colloidal stability [15 and ref. therein]. One uses different approaches to overcome that problem, and the most reliable approach is to create the ligands stabilizing NPs being similar to the structure of liquid crystal molecules [15, 16-21]. One of the most interesting types of liquid crystals is chiral nematic (N*) group. To create N* liquid crystals one needs either to have nematic liquid crystals having chiral centre within the molecules or nematic liquid crystals doped with chiral non-mesogenic molecules capable of creating the nematic twisted structure [22, 23]

The major goal of this paper is to create a new liquid crystal having chiral structure and to analyze the capabilities of those molecules to serve as chiral dopants for a nematic liquid crystal and to provide chiral shell at the surface of nanoparticles that could ensure their strong interaction a LC matrix.

**Materials and methods**

All commercially available starting materials, solvents and reagents were obtained from Acros, Sigma-Aldrich and Merck. The confirmation of the structures of the intermediate and final products was obtained using $^{1}$H NMR spectroscopy (Bruker Avance – 400 MHz), $^{13}$C NMR spectroscopy (Bruker Avance – 500 MHz), elemental analysis

(EuroVector EA3000 Analyzer) and IR spectroscopy (Nicolet 5700, Thermo Fisher Scientific). The thermal properties of the blends were investigated using differential scanning calorimeter Mettler TA-4000 equipped with a DSC-30 heating cell (Mettler Toledo, Switzerland) at a heating rate of 10 K/min under argon. Optical observations were made using a polarizing microscope Polam L-213 (LOMO, St.Petersburg, Russia) equipped with a Mettler Toledo FP-82 HT hot stage and a microprocessor temperature control unit. The temperature of the tested samples was maintained with an accuracy of up to 0.1°C.

***Synthesis of R-MPA***

R-MPA(1)) was prepared from the corresponding 3,6-disubstituted cyclohex-2-enone (4) according to published methods [24-26] . The schema of the synthesis of mesogenic-like R-MPA is given in Figure 1.

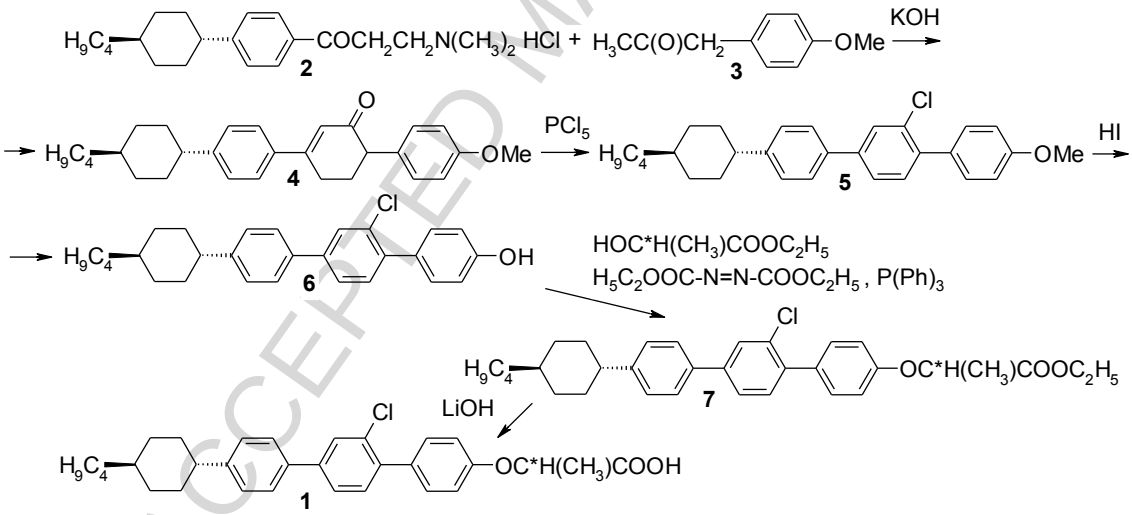


Figure 1. Scheme of the synthesis of (*R*)-2-[4”-(*trans*-4-butylcyclohexyl)-2’-chloro-*p*-terphenyl-4-oxy)propanoic acid (**1**)

Ethyl ester of R-MPA (**7**): 0.1 mol of 4''-(trans-4-Butylcyclohexyl)-2'-chloro-4-hydroxyterphenyl (**6**), 0.11 mol ethyl ester of *L*-lactic acid and 0.12 mol of triphenylphosphine were dissolved in 200 ml of dry THF and cooled to 0°C. Then, 0.12 mol of diethyl azodicarboxylate were added in small portions at 0°C. The mixture was allowed to stir overnight at room temperature. THF was then distilled out in vacuo and the product was purified by column chromatography on silica gel (eluent petroleum ether-ethyl acetate: 10:1), yield 75%.

$^{1}$H NMR ($\delta$, *ppm*, $CDCl_3$):7.67 (1H, d, *J*=1.9 Hz, $H^{3'}$-Ar-*o*-Cl), 7.52 (2H, d, *J*=8.3 Hz, $H^{2''}$,$H^{6''}$-Ar-*m*-Ch), 7.49 (1H, dd, *J*=8.0 Hz, *J*=1.9 Hz, $H^{5'}$-Ar-*p*-Cl), 7.41 (2H, d, *J*=8.7 Hz, $H^{3}$,$H^{5}$-Ar-*m*-OCH),7.36 (1H, d, *J*=8.1 Hz, $H^{6'}$-Ar-*m*-Cl), 7.30 (2H, d, *J*=8.3 Hz, $H^{3''}$,$H^{5''}$-Ar-*o*-Ch), 6.94 (2H, d, *J*=8.8 Hz, $H^{2}$,$H^{6}$-Ar-*o*-OCH), 4.80 (1H, q, *J*=6.8 Hz, O-CH($CH_3$)COO), 4.25 (2H, q, *J*=7.1 Hz, $CH_3$-$CH_2$-O), 2.51 (1H, tt, *J*=12.0 Hz,*J*=3.0 Hz, $CH_{Ch}$-Ar), 1.97-1.85 (4H, m), 1.71 (3H, d, *J*=6.8 Hz, $CHCH_3$), 1.54-1.42 (2H, m), 1.36-1.19 (H, m), 1.27 (3H, t, *J*=7.1 Hz, $CH_3$-$CH_2$-O), 1.13–1.01 (2H, m), 0.91 (3H, t, *J*=7.0 Hz, $CH_3$-$CH_2$).

R-PMA : 0.1 mol of ethyl ester of (7) was dissolved in a mixture of 30 ml of THF, 30 ml of ethyl alcohol and 5 ml of water. Then, 0.15 mol of LiOH was added and stirred at room temperature for 12 hours. The reaction mixture was diluted with water, acidified to pH = 6. The product was extracted with dichloromethane. The extract was dried with anhydrous sodium sulfate. Dichloromethane was evaporated. The expected product is obtained as yellow oil, yield 81%.

$^{1}$H NMR ($\delta$, *ppm*, $CDCl_3$):7.67 (1H, d, *J*=1.9 Hz, $H^{3'}$-Ar-*o*-Cl), 7.52 (2H, d, *J*=8.3 Hz, $H^{2''}$,$H^{6''}$-Ar-*m*-Cl), 7.50 (1H, dd, *J*=8.0 Hz, *J*=1.9 Hz, $H^{5'}$-Ar-*p*-Cl), 7.43 (2H, d, *J*=8.7 Hz, $H^{3}$,$H^{5}$-Ar-*m*-OCH),7.36 (2H, d, *J*=8.1 Hz, $H^{6'}$-Ar-*m*-Cl), 7.30 (2H, d, *J*=8.3 Hz, $H^{3''}$,$H^{5''}$-Ar-*o*-Alk), 6.97 (2H, d, *J*=8.7 Hz, $H^{2}$,$H^{6}$-Ar-*o*-OCH), 4.87 (2H, q, *J*=6.8 Hz, O-$CH(CH_3)$COOH), 2.52 (1H, tt, *J*=12.0 Hz, *J*=3.0 Hz, $CH_{Ch}$-Ar), 1.97-1.85 (4H, m), 1.71 (3H, d, *J*=6.8 Hz, $CHCH_3$), 1.54-1.42 (2H, m), 1.36-1.19 (H, m), 1.13-1.01 (2H, m), 0.91 (3H, t, *J*=7.0 Hz, $CH_3$-$CH_2$).

$^{13}$C NMR (126 MHz, $CDCl_3$) δ = 14.3, 18.6, 23.2, 29.4, 33.7 (2C), 34.5 (2C), 37.3, 37.4, 44.4, 72.3, 114.8 (2C), 125.5, 127.0 (2C), 127.6 (2C), 128.4, 131.0 (2C), 131.7, 132.90, 132.92, 137.0, 138.3, 141.6, 147.9, 156.9, 177.9.

Elemental analysis data**:** Found**, %: C, 75.82; H, 7.19.** $C_{31}H_{35}ClO_3$. Calculated, %**: C,** 75.86; **H, 7**.14.

***Synthesis of CdSe NPs.***

The synthesis of CdSe NPs was carried out in accordance with the procedure used by [27]. In a 100 mL three-necked round-bottom flask 3 mmol of cadmium oxide, 10 mL of octadecene, and 6 mmol of oleic acid were mixed. The mixture was heated under an argon atmosphere to 200$^{o}$C for 1.5 h. The temperature was increased up to 230$^{o}$C, and 3 mL of a 1 molar selenium solution in trioctylphosphine was injected rapidly upon vigorous stirring. The reaction mixture was kept continuously stirring for another 20 min. After that the heating was stopped and the reaction mixture was rapidly cooled down to room temperature. The reaction mixture was transferred into several glass vials and a 3-fold excess of acetone/toluene mixture (2:1) was added. The vials were

centrifuged at 6000 rpm for 5 min to obtain a precipitate. This precipitate was separated followed by subsequent removal of the supernatant and then washed twice with acetone/toluene mixture and centrifuged again. Then the particles were separated, dried under an argon atmosphere and solubilized in hexane. The TEM image of CdSe NPs covered with oleic acid is given in Figure 2.

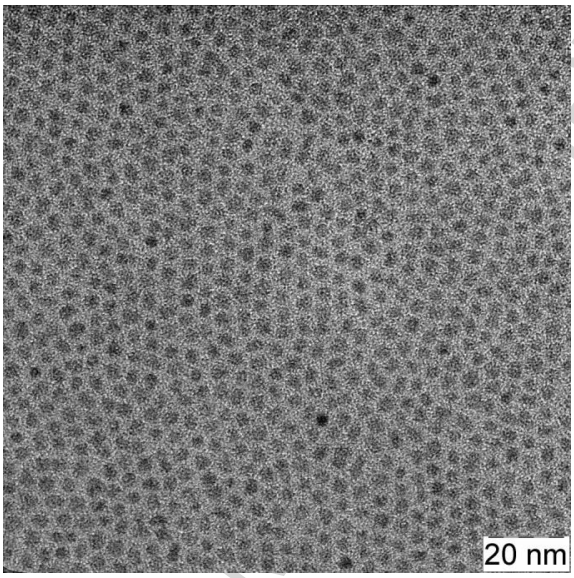


Figure 2. TEM image of synthesized CdSe NPs having 3.5 nm in diameter

***Substitution of the oleic acid at NP's surface by R-MPA.*** The solution of R-MPA of 0.015 g/ml concentration was prepared in toluene. CdSe sol was added in the amount that provided a 50-fold excess relatively to the mass of the aromatic acid. The mixture was kept at room temperature for 24 hours under vigorous

stirring. Then, a 3-fold volume excess of acetone was added and, the mixture was centrifuged at 6000 rpm for 10 min. The precipitate was separated. The above procedure was repeated for several times until the silica gel sorbent stopped to show any

signatures of aromatic acid in the supernatant. The precipitate was dried under argon and dissolved in toluene.

**Results and discussion**

The choice of that compound is dictated by the following reason: several chiral lactic acid derivatives have been studied before [25, 26] and their liquid crystal structure was proven. We have reported in [25] on the synthesis of derivatives of natural chiral *L*-lactic acid namely by the interaction of the corresponding substituted hydroxy-biphenyls, hydroxyterphenyls and hydroxyquaterphenyls with (-) ethyl *L*-lactate.

***Properties of R-MPA.***

The DSC curve of R-MPA is given in Fig.3 (curve 1). This compound shows pretty complex thermal behavior.

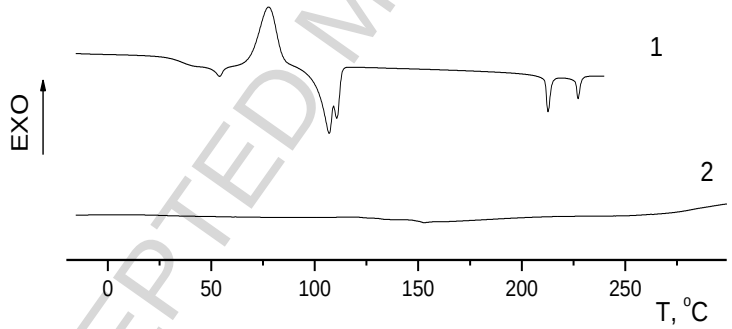


Figure 3. DSC curves of R-MPA (1) and CdSe NPs surface modified by R-MPA (2)

It is not crystallized after the cooling from the isotropic melt and upon heating one can see the glass transition at about 40°C followed by the peak of the crystal formation. Two melting peaks at 108 and 113°C correspond to crystal-crystal and crystal – LC

transitions. In the wide temperature range between 113 and 213ºC the polarized optical microscope (POM) image indicates the confocal texture of a smectic liquid crystal (Fig. 4a) which is transformed into the chiral nematic phase above 213ºC with a characteristic oil strips texture (Fig.4b). The latter melts forming isotropic phase at 230ºC.

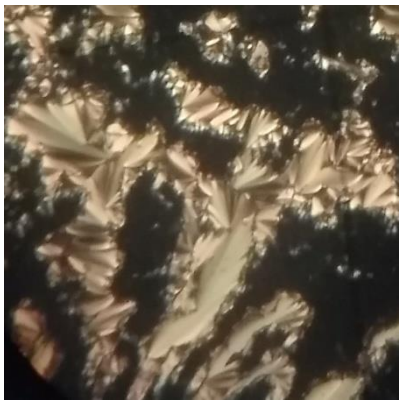
a


b

Figure 4. POM images (crossed polarizers) of R-MPA in the smectic (a) at 150 ºC and chiral nematic phases (b) at 225 º C under heating and cooling

***R-MPA as a dopant***

To check the capability of R-MPA as a dopant inducing the chiral twisting of a nematic phase we have prepared its mixtures with a nematic liquid crystal (NML). This nematic liquid crystal is a mixture of three derivatives of 4-cyanobiphenyl, namely, 4-pentyl-4'-cyanobiphenyl, 4-alkoxy-4'-cyanobiphenyl and 4-cyano-4'-biphenyl ester of trans-4-butylcyclohexanecarboxylic acid.

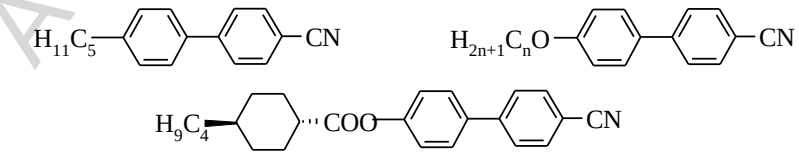

The introduction of up to 30 wt.% of R-MPA shows that the mixture is homogeneous and the N*-I transition temperature ($T_{N^*I}$) increases (Fig.8).

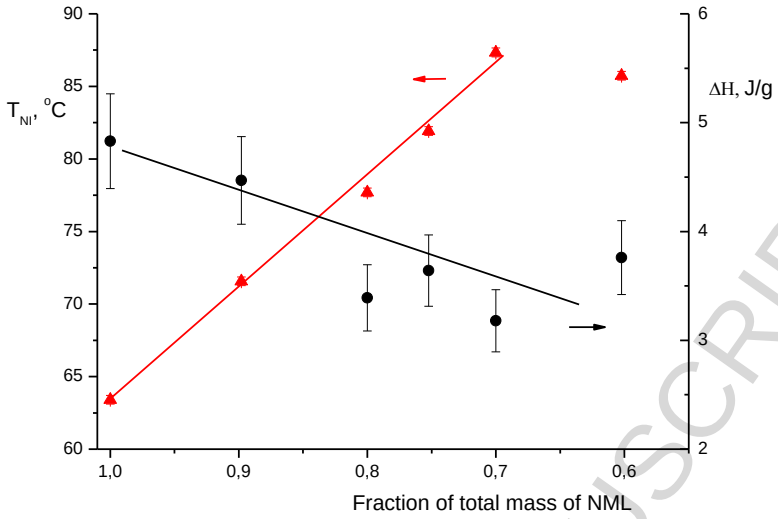


Figure 5.$T_{N^*I}$ (Δ) and the enthalpy (●) of the corresponding phase transition of NML mixed with R-PMA as a function of NML content

Contrary to the previous system there is a strong increase in T resulted from the pretty broad temperature range of the LC phases in R-MPA and the existence of the chiral nematic phase N* between 213 and 230°C. It is necessary to note that the incorporation of the large anisotropic molecules in a nematic liquid crystal may be considered in the zeroth approximation as an addition of anisotropic NPs in a liquid crystal medium. In accordance with the model predictions described in [14] for anisotropic NPs we have expected the enhancement of $T_{NI}$ at homogeneous conditions with the increase in the content of NPs which is experimentally observed.

As for the chiral effect of R-MPA when added in NML, the typical UV-vis spectra of the mixture, containing 22.5-30 wt.% R-MPA indicate the presence of the stop band confirming the chiral twisting of the nematic structure by molecules of R-MPA. One of examples of the absorption spectra of the mixture of NML with 27.5 wt.% of R-MPA at different temperatures is given in Figure 6. There is a shift of the stop band towards the blue spectrum range upon the cooling (Fig. 6a). One can see that the higher is the content of the chiral molecules the lower the wave length of the stop band is which corresponds directly to the smaller helix pitch. The chiral nematic mixtures also show specific thermal behavior of the helix pitch. An unwinding of the helix occurs with the increasing temperature several degrees below $T_{N^*I}$ and after that the stop band does not change any more (Fig. 6b).

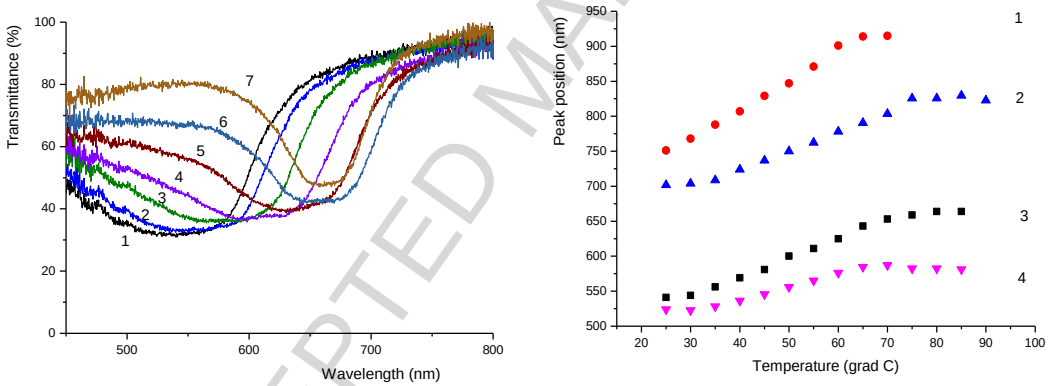


a) b)

Figure 6. Transmittance spectra of the nematic + 27.5 wt. % R-MPA mixture at different temperatures (a) (1-25$^{o}$ C, 2-35 $^{o}$ C, 3-45 $^{o}$ C, 4-55 $^{o}$ C, 5-65 $^{o}$ C, 6-75 $^{o}$ C, 7-85 $^{o}$C) and the stop band position as a function of mixture composition and temperature (b) (1-22.5 wt.%, 2-25 wt.%, 3-27.5 wt.%, 4-30 wt.%)

Such a behavior reminds the pre-transitional phenomena at the chiral nematic – isotropic phase transition described in [29].Though there is no solid explanation for the increase in the stop band wavelength with increasing temperature one can say that the helix formation is due to a balance between the mesogenic interactions tending to untwist the helix structure and twist - forming interactions provided by chiral groups. Between 70 and 25ºC the twisted packing may prevail over mesogenic interactions and it means that the twisted arrangement prevails with the lowering temperature resulted in the smaller helix pitch. Between 70º and clearing point two types of interactions become more or less equal and the pitch does not change until the liquid crystal structure disappears due to the transition of a liquid crystal to the isotropic state. Note that the system discussed about contains R-MPA dopant which is also a liquid crystal on its own having complex thermal history which makes the pictures of interactions even more complicated. The thermal behavior of the induced helix is practically the same except the changing $T_{NI}$. Thus the above results prove the chiral twisting activity of R-MPA. The next step is to check whether the carboxylic group is active for the interaction with the surface of NPs.

***Coating of NPs with R-MPA***

With the goal of placing chiral carboxylic acid ligands R-MPA on the surface of CdSe NPs via postsynthetic ligand exchange, we synthesized CdSe NPs with carboxylate bound oleic acid fragment as described in [25].

The comparison of the IR spectrum of the surface-modified NPs with oleic acid (Fig.7, 1) with the spectrum of R-MPA (2) and CdSe NPs modified by R-MPA (3) after the ligand exchange shows the following. There is a spectral band $\nu_{CO}$ in the spectrum of NPs stabilized by oleic acid at 1538 $cm^{-1}$ that can be referred to an ionic form $COO^-$ and a small band at 720 $cm^{-1}$ corresponding to pendulum oscillation of $CH_2$ groups in polymethylene chains (number of $CH_2$ groups >6) . Those bands allow for the identification of oleic acid moieties at the NP surface. After the treatment of NPs with R-MPA the above IR spectrum (1) undergoes significant changes (2). The comparison of spectra 1 and 2 shows that at the surface of CdSe NP the oleic acid ligands are replaced by R-MPA molecules. The intense band at 1720 $cm^{-1}$ ($\nu_{CO}$) in the spectrum of R-MPA acid (3) indicate that the carboxylic group disappears due to interactions with NPs (spectrum 2) and the new peak appears at 1540 $cm^{-1}$ which is related to $\nu_{CO}$ in the carboxylate ion. In total one can conclude that the ligand exchange reaction resulted in the coating of NPs with R-MPA via ionic interaction presumably with $Cd^{+2}$ at the surface of NPs. As it comes from the DSC curve 2 presented in Figure 3 the solid NPs coated by R-MPA do not show any phase transitions similar to those of R-NMA itself (Figure 3, curve 1).

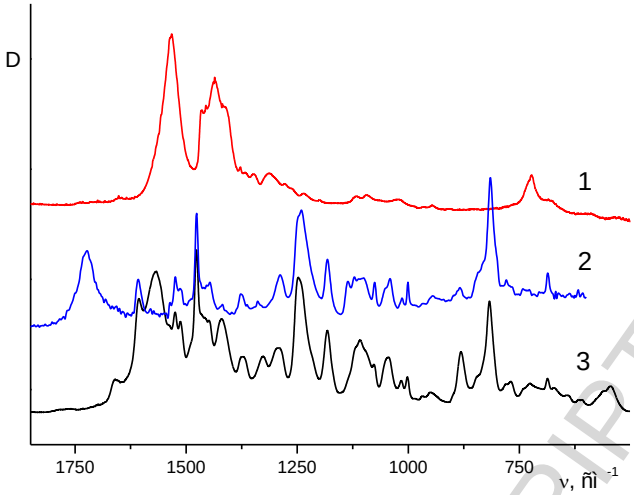


Figure 7 Fourier IR spectra of CdSe NPs, stabilized by oleic (1) and R-MPA (3) acids and the matrix of R-MPA (2)

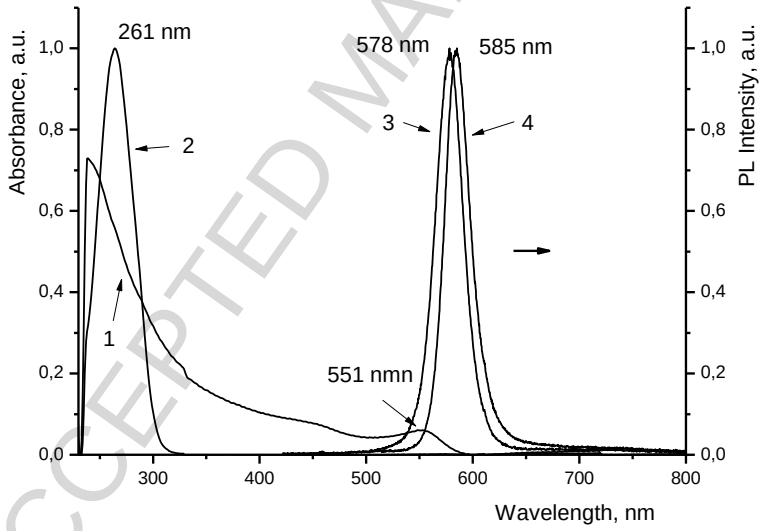


Figure 8. Absorption (1,2) and photoluminescence (3,4) spectra of CdSe NPs stabilized by oleic (1,4) and R-MPA (2,3)) acids in toluene ($\lambda_{ex}$=405 nm).

Absorption spectra change due to the ligand exchange (Figure 8), because R-MPA ligand has an aromatic structure (2) and the oleic acid ligand has no benzene cores in its structure (1). As for photoluminescence spectra the maximum after ligand exchange shifts from 585 nm down to 578 nm. The latter may result from the redistribution of energy at the contact between NP and the ligand.

***R-MPA coated NPs embedded in liquid crystals***

If CdSe NPs stabilized by R-MPA ligands are embedded in R-PMA liquid crystal the thermal and thermodynamic behavior of the system are expected to change. In Figure 9 we show representative DSC scans of the R-MPA doped with CdSe NPs of different concentrations upon heating. The variation of the transition temperatures related to the N*– I and S- N* phase transitions is presented in Figure 10a. We have shown before in [28] that the addition of spherical NPs to nematic liquid crystals leads to the decrease in nematic-isotropic transition temperature ($T_{NI}$) which may be explained by the dilution effect consistent with the theory developed by Osipov and Gorkunov in [14].

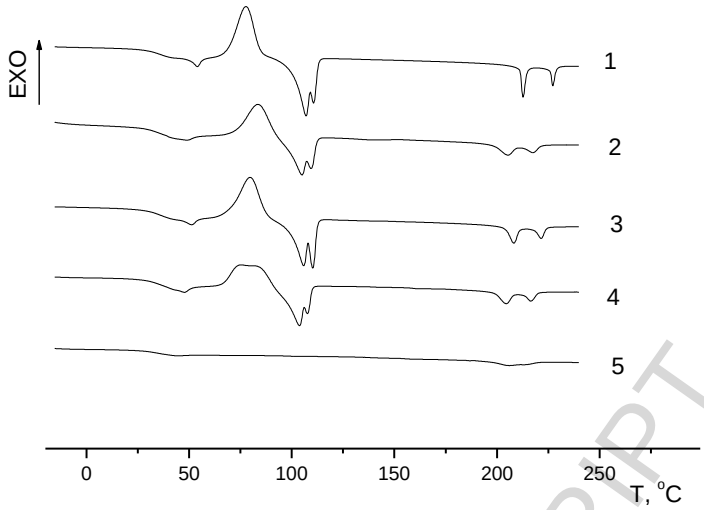


Figure 9. DSC scans of R-MPA doped with different concentrations of NPs stabilized by R-MPA: 1 - 0%, 2 - 0.1, 3 - 1, 4 - 10, 5 – 50 wt.%

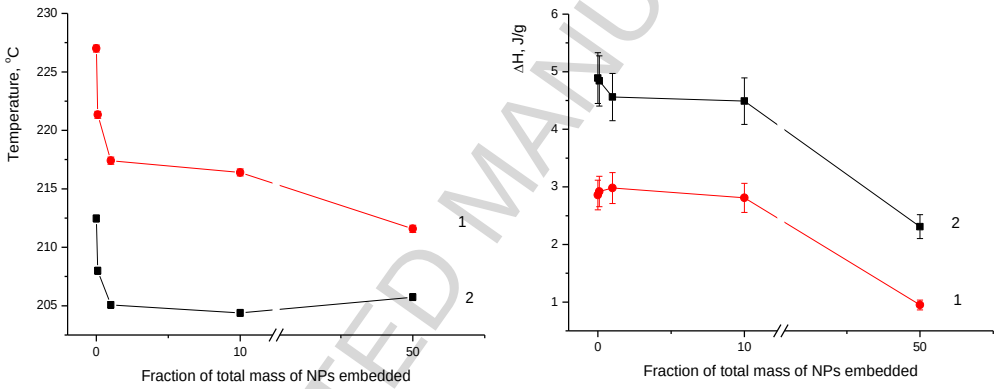


a) b)

Figure 10. Transition temperatures (a) and enthalpies (b) of R-MPA varied with the change in the content of NPs in wt.% embedded into LC matrix : 1- N*-I, 2 – S-N*

The doping of the R-MPA matrix with R-MPA-functionalized NPs results in the qualitatively similar behavior of $T_{N^*I}$ , which is decreased with the increasing contents of NPs (Fig 7a). Note that $T_{SN^*}$ shows the same tendency. Both transition temperatures profiles $T_{N^*I}$ and $T_{SN^*}$ may be split into several intervals of NPs concentrations. A

noticeably strong drop of the transition temperature $T_{N^*I}$ is seen below at 0.01 of the total mass fraction of NPs. The next part of the $T_{N^*I}$ profile is characterized by a much smaller slope in $T_{N^*I}$ at higher NPs concentrations and there is a plateau of the width at about 0.01 – 0.1 of the total mass fraction of NPs. After such an approximately constant level region of $T_{N^*I}$ the transition temperature continues to decrease with the increasing concentration of NPs, but at a much lower rate. As far as the transition enthalpy ($\Delta H_{N^*I}$) is concerned, its change with the increase in the concentration of NPs (Figure 7b) again looks like the 2 stage process. At fairly low NPs content where $T_{N^*I}$ drops down, the enthalpy practically does not change. The plateau region corresponds to the same concentration range where $T_{N^*I}$ is also approximately constant and after that $\Delta H_{N^*I}$ decreases. The profiles of the change in $T_{N^*I}$ and $\Delta H_{N^*I}$ and in $T_{SN^*}$ and $\Delta H_{SN^*}$ with the increase in the content of NPs are very similar, although S-N* phase transition proceeds at the higher temperatures.

However, despite the qualitative similarity with our prior results [26] there exists a considerable quantitative difference. Instead of the small initial drop of about 1-3 degrees of $T_{NI}$ the current system shows thirteen degrees drop, which is unusually large and exceeds the theoretical estimates. The rate of change in the transition temperature is also much larger than the one predicted by the theory. At present the origin of such a strong depression of the transition temperature is not clear although one may conclude that it cannot be explained by the dilution effect alone. Apparently the orientational order of mesogenic molecules is destabilized in the vicinity of the NP.

How do R-MPA coated NPs behave being embedded in the nematic liquid crystal? One can readily see from Figure 11 that the transition enthalpy is decreasing with the increasing concentration of NPs. This decrease in the transition enthalpy is at least partially related to the effect of dilution of the nematic phase by isotropic NPs. On the other hand the transition enthalpy is decreasing faster than the fraction of the mesogenic molecules and hence the decrease cannot be explained by the complete separation between the nematic and the NPs. For example, the transition enthalpy of the composite which contains about 50 wt. % of NPs is 30% less than the values obtained assuming a complete separation between the nematic and the NPs. Thus one may assume that the system separates into the isotropic phase enriched with NPs and the nematic phase which still contains some fraction of NPs. These NPs partially destabilize the orientational ordering which results in the decrease of the nematic order parameter S.

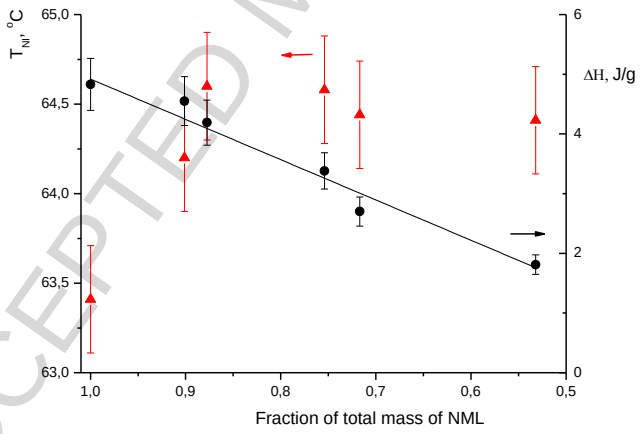


Figure 11. $T_{N^*I}$ (Δ) and the enthalpy (●) of the corresponding phase transition of NML mixed with CdSe NPs stabilized by R-MPA ligands as a function of NML content

One notes that it is sufficient to assume that the nematic order parameter decreases by 10-15 percent to explain the experimental data taking into consideration that the transition enthalpy is approximately proportional to the square of the order parameter S.

The increase in $T_{N^*I}$ may be caused by the shape anisotropy of the NPs. We assume that the anisotropically shaped NPs consist of a quasi - spherical core and anisotropic R-MPA ligand shell. The anisotropy of the ligand shell may result from the interaction between the ligand and LC matrix inducing the deformation of the sphere - like shape of the shell toward the ellipsoidal one (Fig.12).

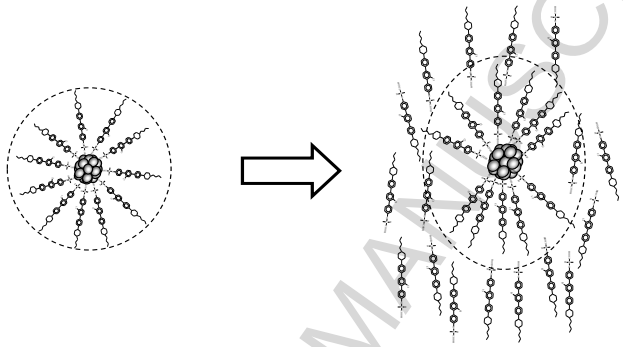

Figure 12. Schematic presentation of the ligand shell transformation in a nematic medium

Note that Mori *et al.* [30] has discussed the similar effect in nematic liquid crystals but filled in with gold NPs stabilized by chiral ligands.

**Conclusions**.

Mesogenic-like acid, (*R*)-2-[4”-(*trans*-4-butylcyclohexyl)-2’-chloro-*p*-terphenyl-4-oxy) propanoic acid (R-MPA), is synthesized and studied. On one hand, it forms a liquid crystal possessing smectic and chiral nematic phase. On the other hand, it is shown to

act as a chiral dopant if added to a conventional nematic system providing the formation of the chiral nematic phase. Finally the same acid can be placed as a ligand at the surface of CdSe NPs. As a dopant R-MPA makes the interval of the chiral nematic phase much broader in comparison with the initial nematic phase. The change in the content of R-MPA allows one to control the helical pitch as it is known for conventional chiral dopants. Spherical CdSe NPs modified by anisotropic mesogenic-like ligands behave as anisotropic NPs being placed in a conventional nematic liquid crystal. The thermodynamics of the nematic-isotropic phase transition is in a good qualitative agreement with the theoretical predictions of Osipov-Gorkunov model [14]. If such NPs are embedded in a liquid crystal phase of R-MPA, we observe the dilution effect predicted for spherical NPs in a nematic medium even though the temperature change is much higher than expected. The observed quantitative inconsistency may result from the identity of NPs ligands and the molecules of the LC medium contributing in a much stronger distortion of a liquid crystal by NPs.

**Acknowledgements**

This work was carried out within the State Program of TIPS RAS. The contribution of Center for molecule composition studies of INEOS RAS is gratefully acknowledged.

REFERENCES

[1] J. Mirzaei, M. Reznikov, T. Hegmann. Quantum dots as liquid crystal dopants. J. Mater. Chem. **22** (2012) 22350–22365. DOI: 10.1039/C2JM33274D

[2] H. Qi, T. Hegmann. Impact of nanoscale particles and carbon nanotubes on current and future generations of liquid crystal display. J. Mater. Chem. 18 (2008) 3288-3294. DOI: 10.1039/B718920F

[3] Y. Shiraishi, N. Toshima, K. Maeds, H. Yoshikawa, J. Xu, S. Kobayashi. Frequency modulation response of a liquid-crystal electro-optic device doped with nanoparticles. Appl. Phys. Lett. 81 (2002) 2845 – 2859

[4] S. Kobayashi., N. Toshima. Nanoparticles and LCDs: It's a surprising world SID. Inf. Display 23 (2007) 26–32.

[5] S.Khatua, P. Manna, W-Sh. Chang, A. Tcherniak, E. Friedlander, E. R. Zubarev, S. Link. Plasmonic nanoparticles-liquid crystal composites. J. Phys. Chem. C 114 (2010) 7251–7257.

[6] H. Yoshida, K. Kawamoto, H. Kubo, T. Tsuda, A. Fujii, S. Kuwabata, M. Ozaki. Nanoparticle-dispersed liquid crystals fabricated by sputter doping. Adv. Mater. 22 (2010) 622-626

[7] E. B. Barmatov, D. A. Pebalk and M. V. Barmatova. Influence of silver nanoparticles on the order parameter of liquid crystalline polymers. Liq. Cryst. 33 (2006) 1059- 1063.

[8] K.K. Vardanyan, A. Daykin, B. Kilmer. Study on cyanobiphenyl nematic doped by silver nanoparticles. Liq. Cryst. 44 (2017) 1240 -1252.

[9] L.A. Bulavin, L.N. Lisetski, S.S. Minenko, A.N. Samoilov, V.V. Klepko, S.I. Bohvan, N.I. Lebovka. Microstructure and optical properties of nematic and cholesteric liquid crystals doped with organo-modified platelets. J. Molecular Liq. 2018. 267 , 279–285

[10] Daniel Budaszewski, Agata Siarkowska, Miłosz Chychłowski, Bartłomiej Jankiewicz, Bartosz Bartosewicz, Roman Dąbrowski, Tomasz R. Woliński. Nanoparticles-enhanced photonic liquid crystal fibers . J. Molecular Liq. 267 (2018) 271–278

[11] P. Kopčanský, N .Tomašovičová, M Koneracká, M .Timko, Z .Mitróová,V. Závišová , N. Éber , K.Fodor-Csorba ,T. Tóth-Katona, A. Vajda , J. Jadzyn, E. Beaugnon , X. Chaud . Structural Phase Transition in Liquid Crystal Doped with Gold Nanoparticles. Acta Phys. Pol. A 118 (2010) 988-989.

[12] G. Sinha, C. Glorieux, J. Thoen. Phys. Broadband dielectric spectroscopy study of molecular dynamics in the glass-forming liquid crystal isopentylcyanobiphenyl dispersed with aerosils. Rev. E: Stat. Nonlinear, SoftMatter Phys. 69 (2004) 031707-031721. DOI:10.1103/PhysRevE.69.031707

[13] T. Bellini, M. Buscagli, C. Chiccoli, F. Mantegazza, P. Pasini and C. Zannoni, Nematics with quenched disorder: What is left when long range order is disrupted?, Phys. Rev. Lett. 31 (2000) 1008-1011. DOI: 10.1103/PhysRevLett.94.097802.

[14] M. V. Gorkunov , M. A. Osipov. Mean-field theory of a nematic liquid crystal doped with anisotropic nanoparticles. Soft Matter 7 (2011) 4348 - 4354.

[15] H. Duran, B. Gazdecki, A. Yamashita, T. Kyu. Effect of carbon nanotubes on phase transitions of nematic liquid crystals. Liq. Cryst. 32 ( 2005) 815-821. DOI: 10.1080/02678290500191204

[16] P Kopcansky, N. Tomasovicova, M. Koneracka, M. Timko, V. Zavisova, A. Dzarova, J. Jadzyn, E. Beaugnon, X. Chaud. Phase Transitions in Liquid Crystal Doped with Magnetic Particles of Different Shapes. Int. J. Thermophys. 32 (2011) 807 -817.

[17] L. M. Lopatina , J. R. Selinger, Phys. Maier-Saupe-type theory of ferroelectric nanoparticles in nematic liquid crystals. Rev. E: Stat., Nonlinear, Soft Matter Phys., 84 (2011) 041703 (7 pages). DOI: 10.1103/PhysRevE.84.041703

[18] M.F. Prodanov, N. V. Pogorelova, A. P. Kryshtal, A. S Klymchenko, Y. Mély, V. P. Semynozhenko, A.I. Krivoshey, Y. A. Reznikov. S. Yarmolenko, J. W. Goodby, V. V. Vashchenko. Thermodynamically Stable Dispersions of Quantum Dots in a Nematic Liquid Crystal. Langmuir 29 (2013) 9301–9309. DOI: 10.1021/la401475b

[19] Marx, V. M.; Girgis, H.; Heiney, P. A.; Hegmann, T. Bent-core liquid crystal (LC) decorated gold nanoclusters: synthesis, self-assembly, and effects in mixtures with bent-core LC hosts. J. Mater. Chem. 18 (2008) 2983–2994.

[20] Qi, H.; Kinkead, B.; Marx, V. M.; Zhang, H. R.; Hegmann, T. Miscibility and Alignment Effects of Mixed Monolayer Cyanobiphenyl Liquid-Crystal-Capped Gold Nanoparticles in Nematic Cyanobiphenyl Liquid Crystal Hosts. Chem. Phys. Chem. 10 (2009) 1211-1218.

[21] Chilaya G.S., Lisetsky L.N. Spiral twisting in cholesteric mesophase. Uspekhi Fizicheskikh Nauk 134 (1981) 279-303.

[22] Dierking I. Chiral Liquid Crystals: Structures, Phases, Effects. Symmetry 6 (2014) 444-472

[23] Brombach F, Neudörfl JM, Blunk D. The Chiral Pool as Valuable Natural Source: New Chiral Mesogens Made From Lactic Acid. Mol Cryst Liq Cryst. 542 (2011) 62-74.

[24] M . Kohout, A.Bubnov, V. Novotná , J. Šturala, J. Svoboda. Effect of alkyl chain length in the terminal ester group on mesomorphic properties of new chiral lactic acid derivatives LC. Liq. Cryst. 43 (2016) 1472-1485.

[25] V.S. Bezborodov, S.G. Mikhalyonok, N.M. Kuz'menok, V.I. Lapanik , G.M. Sasnousky. Polyfunctional intermediates for the preparation of liquid crystalline and anisotropic materials. Liq Cryst. 42 (2015) 1124-1138.

[26] V.S. Bezborodov, S.G. Mikhalyonok, N.M. Kuz'menok, A.S. Arol, G.A. Shandryuk, A.S. Merekalov, O.A. Otmakhova, G.N. Bondarenko, R.V. Talroze.Anisotropic derivatives of (-)- L -lactic acid and their nanocomposites. Liq. Cryst. 45 (2018) 1223-1233

[27] G. A. Shandryuk, E. V. Matukhina, R. B. Vasil'ev, A. Rebrov, G. N. Bondarenko, A. S. Merekalov, A. M. Gas'kov, R.V. Talroze. Semiconductor quantum dots organized by a liquid crystal polymer medium. Macromolecules 41 (2008) 2178-2185

[28] M. V. Gorkunov, G. A. Shandryuk,, A. M. Shatalova. I. Y. Kutergina, A.S. Merekalov, A. S., Y. V. Kudryavtsev, R. V. Talroze, M.Osipov. Phase separation effects and the nematic-isotropic transition in polymer and low molecular weight liquid crystals doped with nanoparticles. Soft Matter. 9 (2013) 3578-3588

[29] J.Lub, D.J. Broer, R.A.M. Hikmet, K.G.J. Nierop. Synthesis and photopolymerization of cholesteric liquid crystalline diacrylates. Liq.Cryst. 18 (1995) 319-326

[30] T. Mori, A. Sharma, and T. Hegmann, Significant Enhancement of the Chiral Correlation Length in Nematic Liquid Crystals by Gold Nanoparticle Surfaces Featuring Axially Chiral Binaphthyl Ligands. ACS Nano, 2016, 10 (1), pp 1552–1564

Graphical abstract